

## ARTICLE

Michael Rappolt · Gert Rapp

## Structure of the stable and metastable ripple phase of dipalmitoylphosphatidylcholine

**Abstract** Dipalmitoylphosphatidylcholine (DPPC) dispersed in excess water forms a stable ripple phase upon heating from the gel phase and a metastable ripple phase  $P_{\beta'}$  (mst) upon cooling from the liquid crystalline phase. The X-ray diffraction pattern of  $P_{\beta'}$  (mst) displays several reflections in the range from  $1/25$  to  $1/2.8 \text{ nm}^{-1}$ , which can all be indexed on a two-dimensional monoclinic lattice (space group  $p2$ ) with  $a=26.2$ ,  $b=8.63 \text{ nm}$  and  $\gamma=107^\circ$ . In contrast to the stable ripple phase, which shows a sawtooth like surface profile and an almost constant bilayer thickness, the electron density map of the metastable ripple phase shows an almost symmetric surface profile with a modulation length of  $26.2 \text{ nm}$ . The lipid bilayer thickness varies from  $3.9$  to  $4.4 \text{ nm}$ , which most likely arises from a continuous periodic change of the tilt of the chains to the surface normal of between  $30$  and  $40$  degrees. A further important feature of the structure is the staggered stacking of the bilayers with water pockets enclosed.

**Key words** X-ray diffraction · Ripple phase · Lecithin · Martensitic transformation · Membrane

### Introduction

In aqueous dispersions of dipalmitoylphosphatidylcholine (DPPC) a so-called ripple phase forms at  $35^\circ\text{C}$  upon heating from the lamellar gel phase ( $L_{\beta'}$ ). At the main transition at  $42^\circ\text{C}$  it converts into the liquid crystalline ( $L_{\alpha}$ ) phase (see e.g. Cevc and Marsh 1987). Two existing rippled structures were reported from freeze fractured liposomes of DMPC (Ververgaert et al. 1972) showing two bands with spacings of  $11.7$  and  $23.3 \text{ nm}$ , respectively. A short rippled structure, and one about twice as long, were confirmed in

further freeze etch studies on liposomes of DLPC, DPPC and DSPC (Verkleij et al. 1972; Ververgaert et al. 1973). In a systematic investigation on the appearance of the rippled structures by freeze fracture electron microscopy Luna and McConnell (1977) found that in DMPC and DPPC these form only when the samples are quenched from temperatures between the pre- and main transition.

The conditions for the different ripple phases to appear have been clarified in time-resolved X-ray diffraction studies on DPPC dispersions (Tenchov et al. 1989; Yao et al. 1991). During heating from the lamellar gel phase ( $L_{\beta'}$ ) only the short ripple phase ( $P_{\beta'}$ ) appears while upon cooling from the liquid crystalline ( $L_{\alpha}$ ) phase, both the short and long ( $P_{\beta'}$  (mst)) ripple phases form, with the long ripple phase as the dominating one. The latter exists for at least several hours. It can be readily transformed into the stable, i.e., short ripple phase after cooling the sample below the pretransition temperature to e.g.  $28^\circ\text{C}$  and subsequently reheating through the pretransition (Fig. 1).

The structure of the ripple phase was further investigated using oriented layers of phosphatidylcholines (Alecio et al. 1985). In the formation of the  $P_{\beta'}$  phase from the gel phase Hentschel and Rustichelli (1991) found a change in the hydrocarbon-chain direction. The ripple phase of DMPC was investigated by Zasadzinski et al. (1988) using scanning tunneling microscopy. They found a ripple wavelength of about  $12 \text{ nm}$  which is a typical value for the stable ripple phase, although from their preparation the metastable ripple phase should be expected.

The electron density profile of the stable ripple phase of DLPC has been known from X-ray diffraction studies (Tardieu et al. 1973). The structure of the metastable  $P_{\beta'}$  (mst) ripple phase, however, is hitherto unknown. In the present X-ray diffraction study on aqueous dispersions of DPPC twelve reflections of the metastable  $P_{\beta'}$  (mst) ripple phase were observed which can all be indexed on a two-dimensional monoclinic lattice. By symmetry considerations  $64$  possible phase combinations remained from the original  $4096$ . Electron density maps were calculated using the observed intensities and all possible phase combinations.

M. Rappolt · G. Rapp (✉)  
European Molecular Biology Laboratory,  
Hamburg Outstation c/o DESY, Notkestrasse 85,  
D-22603 Hamburg, Germany  
(Fax: +49-40-89902 149, e-mail: rapp@embl-hamburg.de)

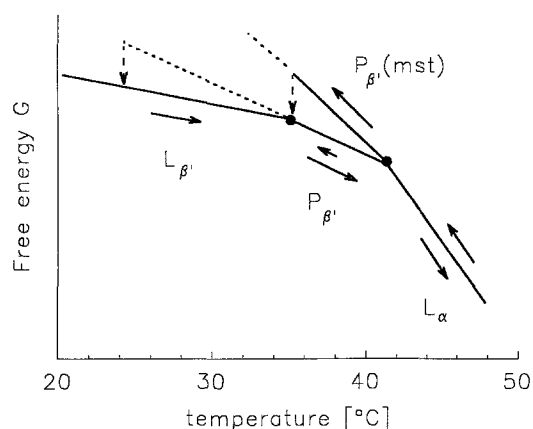


**Fig. 1** Free energy representation of aqueous suspensions of DPPC. Heating and cooling pathways are indicated by solid arrows in the stable phases  $L_{\beta'}$ ,  $P_{\beta'}$  and  $L_{\alpha}$  and in the metastable ripple phase  $P_{\beta'}(mst)$ . The metastable ripple phase  $P_{\beta'}(mst)$  forms only upon cooling from the liquid crystalline phase. Dashed lines indicate undercooled phase regions of the two ripple phases

## Materials and methods

### Sample preparation

DPPC (1,2-dipalmitoyl-sn-glycero-3-phosphocholine, purity >99%) from Avanti Polar Lipids, Inc. (Alabaster, AL) was used without further purification. Weighed amounts of lipids (40% w/w) were dispersed in distilled water (Fluka, Neu Ulm: specific resistance 18 M $\Omega$  cm) and incubated at 55 °C for 90 min. Then the samples were repeatedly vortexed and incubated at 55 °C and stored for at least 12 h at 4 °C. A droplet of lipid dispersion was placed in a 5 mm diameter hole of a 600  $\mu$ m thick stainless steel plate and sealed with 12  $\mu$ m thin mylar foil. The plate was placed in a temperature controlled brass block. The samples were investigated at 39 °C after heating through the pretransition and cooling through the main transition, respectively. The actual temperature was measured with a NiCr-Ni thermocouple placed close to the sample.

### X-ray diffraction and experimental protocol

Diffraction patterns were recorded on the X13 double focusing monochromator-mirror camera (Hendrix et al. 1979) of the EMBL Outstation at the Deutsches Elektronen Synchrotron (DESY) in Hamburg on the storage ring DORIS. At this beam line the wavelength is fixed to 0.15 nm. The data acquisition system is described elsewhere (Rapp et al. 1995). The distance from the sample to the linear detector (Gabriel 1977) was 3 m. In this geometry the detector covered the region from (35 nm) $^{-1}$  to (2.75 nm) $^{-1}$ . To minimize the X-ray dose on the sample a fast solenoid driven shutter controlled by the data acquisition system was used to prevent irradiation of the sample

in those periods where no diffraction data are taken. In the experiments an alternating sequence of 60 s exposure time and 30 min waiting time was used. The total exposure time did not exceed 10 min.

Radiation damage was checked by thin layer chromatography (solvent chloroform/methanol/ammonia solution 25%; 65:35:5, by vol). The size and position of single spots of both fresh and irradiated samples were identical and showed not traces of degradation. Further, the diffraction patterns taken in a period of three hours of the metastable phase were compared and showed an intensity profile stable within 3%.

### Data reduction and analysis

X-ray diffraction patterns of the stable and metastable ripple phase, respectively, were background subtracted with polynomial fits and Lorentz corrected. Using a linear detector the Lorentz factor is equal to  $s$  for point collimation and to  $s^2$  for slit collimation ( $s$ : scattering vector  $s = 2 \sin \Theta / \lambda$ ,  $2 \Theta$  = scattering angle,  $\lambda$ : wavelength of X-rays). Since the shape of the focus of the beam line is slightly elliptical, a Lorentz factor of  $s^{3/2}$  was used. This factor was derived from calculations of the electron density profile of DPPC in the gel phase at 20 °C using the first five orders of the diffraction pattern with three different Lorentz corrections:  $s$ ,  $s^{3/2}$  and  $s^2$ , respectively. The criterion applied for the best correction was that in the region of the aliphatic chains the electron density should remain almost constant (Tardieu et al. 1973; Wiener et al. 1989) which was in fact true only if a Lorentz factor of  $s^{3/2}$  was applied.

A difficulty in the determination of the correct amplitudes of the reflections of the metastable phase arises from the fact that during cooling both the stable and metastable ripple phases form. It is therefore necessary to extract the X-ray diffraction pattern of the metastable ripple from the measured pattern originating from a mixture of both stable and metastable phases, respectively. With the assumption that the structure of the stable (short) ripple phase is independent of the pathway of the temperature change, i.e. heating from the gel or cooling from the liquid crystalline phase, and depends only on temperature, it is possible to determine the contributions of either phase to the diffraction pattern. Raw data of the ripple phase obtained after heating from the gel phase and cooling from the liquid crystalline phase, respectively, are shown in Fig. 2. The (10)-reflection at 0.073 nm $^{-1}$  of the stable ripple phase is the only reflection which appears in the joint pattern of stable and metastable phase, respectively, in an angular regime where it does not overlap with other reflections. The intensity of this reflection was used to elucidate the volume fraction of the stable ripple phase within the joint pattern of stable and metastable phase, respectively. The diffraction pattern of the stable ripple phase was scaled using the intensity of the (10)-reflection at 0.073 nm $^{-1}$  and subtracted from the diffraction pattern obtained during cooling. This procedure is applicable since the (20)-reflec-

tion of the metastable phase does not coincide with the (10)- reflection of the stable phase. In our experimental set-up the reflections would be separated on the detector by 12 channels, equivalent to  $0.008 \text{ nm}^{-1}$ . Further, the widths of the (10)-reflections in both patterns are similar ( $\text{HWHM}=0.0025 \text{ nm}^{-1}$ ) indicating that there is no (20)-reflection present at this water concentration. The error in the scaling factor which originates from the weak intensity of the (10)-reflection causes errors in the amplitudes of the extracted pattern of the metastable ripple phase between 8 and 25%.

The reduced data were fitted by a least-squares method based on the Levenberg-Marquardt algorithm. For a review see Press et al. (1986). All overlapping reflections were modelled by a sum of Lorentzians.

### Indexing

The stable ripple phase belongs to space group p2 (Tardieu et al. 1973) which facilitates indexing of the respective reflections. The cell parameters were fitted from the observed spacings (Table 1) of the (10), (01), (11) and (12)-reflections resulting in  $a=13.68 \text{ nm}$ ,  $b=7.21 \text{ nm}$ ,  $\gamma=95.3^\circ$ . The (-11) and (-12)-reflections were taken into account for the fitting procedure.

For the metastable ripple phase Yao et al. (1991) attempted a lattice assignment from their X-ray diffraction data. Indications from freeze fracture electron micrographs led them to the assumption that the diffraction pattern of the ripple phase detected during a cooling scan arises from a superposition of the diffraction pattern from the stable phase with a second one arising from a ripple structure with a rectangular space group. However, as they admitted their indexing was not conclusive. The crucial point is that the approximately twofold wavelength of the secondary ripple structure profile as known from freeze fracture electron microscopy gives no indications for its two dimensional space group since it does not show the stacking geometry of the bilayers. In the present work it is shown that the diffraction pattern of the metastable ripple phase can be indexed perfectly on a monoclinic lattice of space group p2. The cell parameters of this structure (Table 2) were fitted from the observed spacings of the (10), (-11), (01), (11), (21), (31), (-12), (12) and (22)-reflections resulting in  $a=26.19 \text{ nm}$ ,  $b=8.63 \text{ nm}$ ,  $\gamma=107.3^\circ$ . The correlation of the calculated to observed spacings is 0.99996.

### Phase screening and electron density calculation

Space group p2 is centro symmetric with four centers of symmetry, i.e., the phases of two reflections can be fixed. From the fitted amplitudes of the reflections two-dimensional electron density maps of the stable and metastable ripple phase, respectively, were calculated from all possible phase combinations using the program CCP4 (9). No scaling of the density was applied, i.e., the mean density is zero. The correct phase assignment of the reflections was

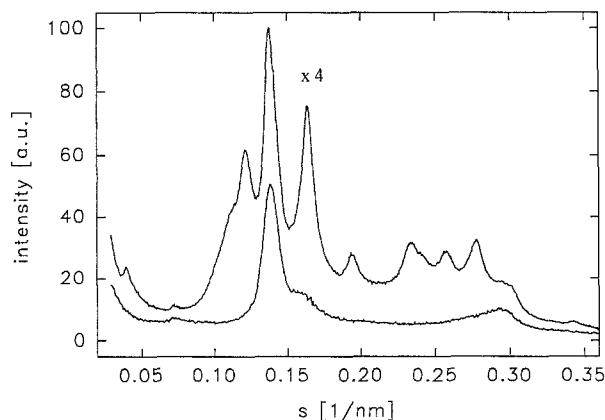


**Fig. 2** Raw X-ray diffraction patterns of the stable (*bottom*) and metastable (*top*) ripple phase

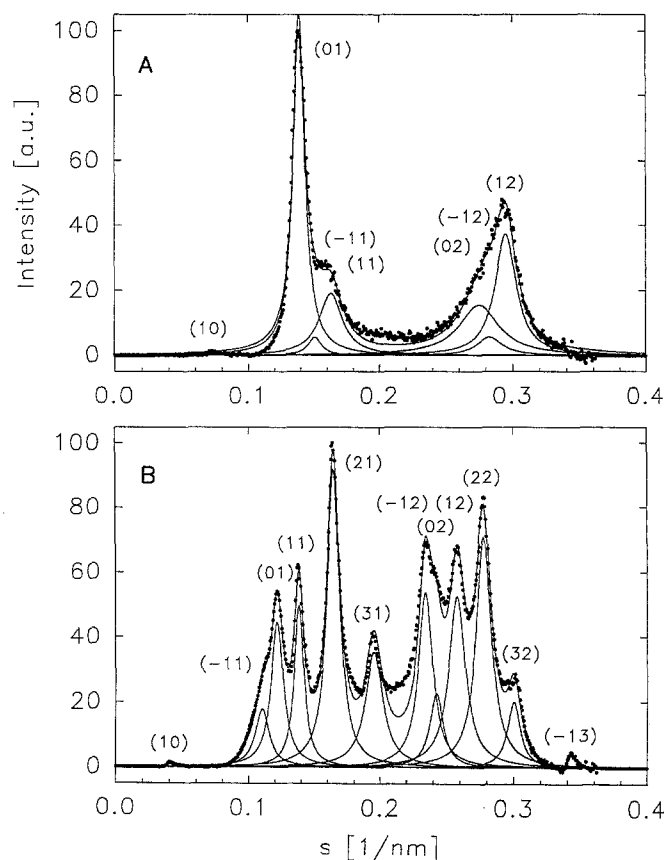


**Fig. 3** Background subtracted and Lorentz corrected X-ray diffraction pattern of (A) the stable ripple phase  $P_{\beta'}$  at  $39^\circ\text{C}$  after heating from the gel phase  $L_{\beta'}$  and (B) the metastable ripple phase  $P_{\beta'}$  (mst) at  $39^\circ\text{C}$  after cooling from the liquid crystalline phase  $L_{\alpha}$ . The experimental data are represented by dots, the solid lines show the fits

elucidated using two protocols. Taking only regions of positive density, i.e., the phospholipid headgroups into account, the calculated density maps were screened for their bilayer properties and sorted into four categories: (i) absence of a bilayer structure, (ii) poor continuity of the bi-

**Table 1** Crystallographic data of the stable ripple phase  $P_{\beta}$ 

| h  | k | $s_{\text{obs}}$ (l/nm) | $s_{\text{calc}}$ (l/nm) | I   | F     |
|----|---|-------------------------|--------------------------|-----|-------|
| 1  | 0 | 0.073                   | 0.073                    | 1.2 | -1.1  |
| 0  | 1 | 0.139                   | 0.139                    | 100 | +10.0 |
| -1 | 1 | *                       | 0.151                    | 6   | -2.5  |
| 1  | 1 | 0.163                   | 0.163                    | 36  | +6.0  |
| 0  | 2 | 0.275                   | 0.279                    | 50  | -7.1  |
| -1 | 2 | *                       | 0.282                    | 12  | +3.5  |
| 1  | 2 | 0.295                   | 0.295                    | 64  | -8.0  |

**Table 2** Crystallographic data on the metastable ripple phase  $P_{\beta}$  (mst)

| h  | k | $s_{\text{obs}}$ (l/nm) | $s_{\text{calc}}$ (l/nm) | I   | F     |
|----|---|-------------------------|--------------------------|-----|-------|
| 1  | 0 | 0.039                   | 0.040                    | 1.0 | -1.0  |
| -1 | 1 | 0.111                   | 0.116                    | 22  | +4.7  |
| 0  | 1 | 0.121                   | 0.121                    | 49  | -7.0  |
| 1  | 1 | 0.138                   | 0.139                    | 42  | +6.5  |
| 2  | 1 | 0.164                   | 0.164                    | 100 | -10.0 |
| 3  | 1 | 0.195                   | 0.194                    | 55  | +7.4  |
| -1 | 2 | 0.234                   | 0.234                    | 26  | -5.1  |
| 0  | 2 | 0.242                   | 0.243                    | 67  | -8.2  |
| 1  | 2 | 0.258                   | 0.257                    | 76  | +8.7  |
| 2  | 2 | 0.278                   | 0.277                    | 92  | -9.6  |
| 3  | 2 | 0.300                   | 0.301                    | 21  | +4.6  |
| -1 | 3 | 0.344                   | 0.354                    | 3   | -1.7  |

layer, (iii) incorrect lipid bilayer thickness and (iv) above criteria fulfilled. Many phase combinations showed isolated, branched or crossed density motifs rather than a bilayer structure. They were easily detected by eye and were rejected. Phase combinations which led to interruptions in the positive density larger than 2 nm fell into the second category and were also rejected. As a constraint for the third category the range of accepted lipid bilayer thickness was set to 3–5 nm, i.e., the range of the lipid bilayer in the liquid crystalline phase and in the gel phase, respectively. Wack and Webb (1989) investigated the lyotropic behaviour of the stable ripple phase of lecithin in great detail and showed that the lipid bilayer thickness shrinks with increasing water concentration. Since the metastable phase forms only upon cooling from the liquid crystalline phase where the lipids are more hydrated than in the gel phase a bilayer thickness larger than that of the gel phase was also excluded for the metastable phase.

In the second protocol one dimensional electron density profiles perpendicular to the bilayer stacking were calculated and screened for bilayer profiles most similar to the one of the ripple structure known from DLPC (Tardieu et al. 1973). The orientation of the trajectories was determined from the Patterson map, i.e., the profiles were calculated along a straight line approximately parallel to the b-axis intersecting the a-axis at the origin or at  $a/2$ . Finally, the model profile was fitted to all possible profiles using the scaling factor and the phase as fit parameters.

The screening of the correct phase combination of the metastable phase was done in two steps. First, the protocols outlined above were applied to all possible phase com-

binations of the seven strongest reflections which led to a unique solution. In the second screening process the weaker reflections were included.

## Results and discussion

### The stable ripple phase

The electron density profile obtained for the stable ripple phase of DPPC (Fig. 4) is very similar to that of DLPC reported earlier (Tardieu et al. 1973). The ripple repeat is 13.7 nm, the profile is asymmetric saw-tooth like with a ratio of about 1/3 of the projected sides to the plane of membrane. This has also been reported from electron microscopy studies on freeze fractured samples of unilamellar vesicles of DMPC (Sackmann et al. 1980). The thickness of the lipid bilayer is almost constant at 4.1–4.2 nm. The conformation of the aliphatic chains of the lipids in the ripple phase is still ambiguous. X-ray diffraction experiments (Tardieu et al. 1973, Janiak et al. 1976) show evidence for an all-trans conformation of the lipid chains although some gauche conformers may be present (Ruocco and Shipley 1982). On the other hand NMR studies indicated that in the  $P_{\beta}$  phase some aliphatic chains adopt a conformation similar to the one in the gel phase and some like the one in the liquid crystalline phase (Wittebort et al. 1981). However, judging from the wide-angle reflections of our own measurement (Rapp et al. 1993) the fraction of lipid molecules with liquid like chains must be very small.

In the gel phase we found a lipid thickness of 4.3 nm at 20 °C. The tilt of the aliphatic chains relative to the membrane normal is 32 ° (Tristram-Nagle et al. 1993). Lipid molecules in the all-trans conformation fit perfectly into the resulting electron density profile of the stable ripple phase provided that the aliphatic chains are tilted about 28 ° to the membrane plane normal. Evidence that the lipid chains are predominantly in the all-trans conformation also in the coexistence range of the stable and metastable phases is provided by analysis of the wide angle reflection at  $1/0.42 \text{ nm}^{-1}$  which arises from the hexagonal packing of the lipid chains and which has the same height and width in both phases.

### The metastable ripple phase

The electron density distribution of the metastable ripple phase is shown in Fig. 5. The surface profile is almost symmetric with a modulation length of 26.2 nm which is substantially different from the one of the stable ripple phase (Fig. 4) where the modulation length is 13.7 nm and the profile is saw-tooth like. The structure is compatible with the results from freeze fracture electron microscopy studies although the grooves reported by Sackmann et al. (1980) for unilamellar vesicles are not observed. However, these grooves may be a peculiarity of unilamellar vesicles. The bilayer thickness varies from 3.9 to 4.4 nm which com-

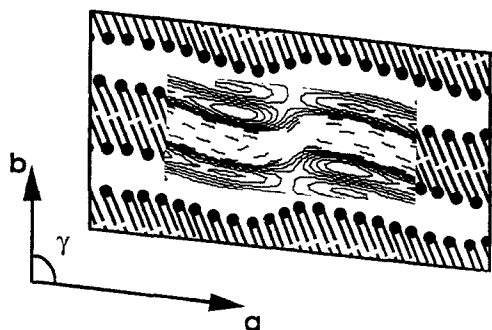


**Fig. 4** Model structure of the stable ripple phase  $P_{\beta}$ . Four unit cells are shown. The *insert* shows the electron density distribution as calculated from the data of Table 1. The lipids are drawn in the all-trans conformation. The saw-tooth like modulation is clearly observable

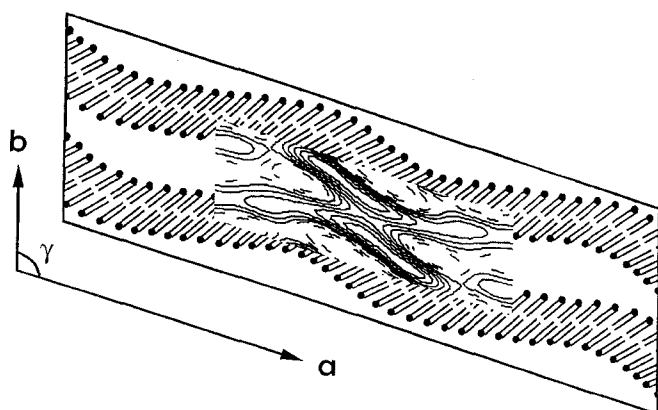


**Fig. 5** Model structure of the metastable ripple phase  $P_{\beta}$ (mst). Four unit cells are shown. The *insert* shows the electron density distribution as calculated from the data of Table 2. The lipids are drawn in all-trans conformation. The structure is characterized by a homogeneous surface and chain tilt angle modulation and enclosed water pockets

compares to 3.5 nm in the liquid crystalline phase. It is therefore again evidence that the lipid chains are predominantly in the all-trans conformation with the consequence that their tilt to the surface normal must vary between  $30^\circ$  and  $40^\circ$  to compensate the changes in the lipid bilayer thickness and consequently lead to lateral pressure fluctuations (Gebhardt and Sackmann 1977).

The variation of the lipid bilayer thickness is consistent with the lyotropic behaviour of the stable ripple phase of lecithin, where the lipid bilayer thickness shrinks with the water concentration (Wack and Webb 1989). Here the bilayer thickness has its maximum thickness at regions of low water content and vice versa. The existence of the water pockets as shown in Fig. 5 leads to the monoclinic lattice of space group  $p2_1$ . It also explains why the structure appears only upon cooling from the liquid crystalline phase. In the metastable ripple phase the amount of water is approximately 30% higher than in the stable phase. This is even more water than in the liquid crystalline phase. It

explains the presence of both the stable phase which has less water than the metastable phase and which thus can form in a more or less diffusionless manner from the liquid crystalline phase. The results support the idea of a martensitic transformation in hydrated phospholipid liquid crystals as proposed by Chan and Webb (1981). They discuss the possibility of an inhomogeneous shear transformation driven by molecular conformational changes. This would generate a two dimensional structure of an almost doubled corrugation period in a second shear, which is very similar to the one we found for the metastable ripple phase. Martensitic transformations in phospholipid phase transitions have also been discussed in context with the results from fast time-resolved X-ray diffraction studies (Laggner and Kriechbaum 1991).

**Acknowledgements** We are grateful to Andrey Lebedev for assistance with the CCP4 program and to Prof. Laggner for critical reading of the manuscript.

## References

- Alecio MR, Miller A, Watts A (1985) Diffraction of X-rays by rippled phosphatidylcholine bilayers. *Biochim Biophys Acta* 815: 139–142
- Chan WK, Webb WW (1981) Possible martensitic transformation in hydrated phospholipid liquid crystals. *Phys Rev Letters* 46:39–42
- Cevc G, Marsh D (1987) *Phospholipid bilayers*. Wiley, New York
- Collaborative Computational Project, Number 4 (1994) The CCP4 Suite: Programs for protein crystallography. *Acta Cryst D* 50:760–763
- Doniach S (1979) A thermodynamic model for the monoclinic (ripple) phase of hydrated phospholipid bilayers. *J Chem Phys* 70:4587–4596
- Gabriel A (1977) Position sensitive X-ray detectors. *Rev Sci Instrum* 48:1303–1305
- Gebhardt C, Sackmann E (1977) On domain structure and local curvature in lipid bilayers and biological membranes. *Z Naturforsch* 32:581–596
- Hentschel MP, Rustichelli F (1991) Structure of the ripple phase  $P_{\beta}$  in hydrated phosphatidylcholine multimembranes. *Phys Rev Lett* 66:903–906
- Janiak MJ, Small DM, Shipley GG (1976) Nature of the thermal pretransition of synthetic phospholipids: dimyristoyl- and dipalmitoyllecithin. *Biochemistry* 15:4575–4580
- Laggner P, Kriechbaum M (1991) Phospholipid phase transitions: kinetics and structural phase transitions. *Chem Phys Lipids* 57:121–145
- Luna EJ, McConnell HM (1977) The intermediate monoclinic phase of phosphocholines. *Biochim Biophys Acta* 466:393–401
- Press WH, Teukolsky SA, Vetterling WT, Flannery BP (1986) *Numerical recipes*. Cambridge University Press, Cambridge
- Rapp G, Rappolt M, Laggner P (1993) Time-resolved simultaneous small- and wide-angle X-ray diffraction on dipalmitoyl-phosphatidylcholine by laser temperature jump. *Prog Colloid Polym Sci* 93:25–29
- Rapp G, Gabriel A, Dosiere M, Koch MHJ (1995) A dual detector single readout system for simultaneous small-(SAXS) and wide-angle X-ray (WAXS) scattering. *Nucl Instrum Meth Phys Res A* 357:178–182
- Ruocco MJ, Shipley GG (1982) Characterization of the sub-transition of hydrated dipalmitoyl-phosphatidylcholine bilayers. Kinetic, hydration and structural study. *Biochim Biophys Acta* 691:309–320
- Sackmann E, Ruppel D, Gebhardt C (1980) Defect structure and texture of isolated bilayers of phospholipids and phospholipid mix-

- tures. In: Helfrich W, Heppke G (eds) Liquid crystals of one- and two-dimensional order. Konferenz Garmisch-Partenkirchen. Springer, Berlin Heidelberg New York, pp 309–326
- Tardieu A, Luzzati V, Reman FC (1973) Structure and polymorphism of hydrocarbon chains of lipids: A study of lecithin-water phases. *J Mol Biol* 75:711–733
- Tristram-Nagle S, Zhang R, Suter RM, Worthington CR, Sun W-J, Nagle JF (1993) Measurement of chain tilt in fully hydrated bilayers of gel phase lecithins. *Biophys J* 64:1097–1109
- Tenchov BG, Yao H, Hatta I (1989) Time-resolved X-ray diffraction and calorimetric studies at low scan rates. I. Fully hydrated dipalmitoylphosphatidylcholine (DPPC) and DPPC/water/ethanol phases. *Biophys J* 56:757–767
- Verkleij AJ, Ververgaert PHJ, Van Deenen LLM, Elbers PF (1972) Phase transitions of phospholipid bilayers and membranes of *Acholeplasma Laidlawii* B visualized by freeze fracturing electron microscopy. *Biochim Biophys Acta* 288:326–332
- Ververgaert PHJ, Elbers PF, Lutingh AJ, Van Den Berg HJ (1972) Surface patterns in freeze-fractured liposomes. *Cytobiology* 6:85–96
- Ververgaert PHJ, Verkleij AJ, Elberts PF, Van Deenen LLM (1973) Analysis of the crystallization process in lecithin liposomes: A freeze-etch study. *Biochim Biophys Acta* 311:320–329
- Wack DC, Webb WW (1989) Synchrotron X-ray study of the modulated lamellar phase  $P_{\beta}$  in the lecithin-water system. *Phys Rev A* 40:2712–2730
- Wiener MC, Suter RM, Nagle JF (1989) Structure of the fully hydrated gel phase of dipalmitoylphosphatidylcholine. *Biophys J* 55:315–325
- Wittebort RJ, Schmidt CF, Griffin RG (1981) Solid-state carbon-13 nuclear magnetic resonance of lecithin gel to liquid-crystalline phase transition. *Biochemistry* 20:4223–4228
- Yao H, Matuoka S, Tenchov B, Hatta I (1991) Metastable ripple phase of fully hydrated dipalmitoyl-phosphatidylcholine as studied by small angle X-ray scattering. *Biophys J* 59:252–255
- Zasadzinski JAN, Schneir J, Gurley J, Elings V, Hansma PK (1988) Scanning tunneling microscopy of freeze-fracture replicas of biomembranes. *Science* 239:1013–1015